RSC Advances

ROYAL SOCIETY OF CHEMISTRY

www.rsc.org/advances

Hydrothermal Growth of Large-Size UO_2 Nano-particles Mediated by Biomass and Environmental Implications

Yangjian Cheng[a,b], *Xinya Xu*[a], *ShungaoYin*[b], *Xiaohong Pa*[b], *Zhi Chen*[b], *and Zhang Lin*[b,*]

a. College of Environment and Resources, Fuzhou University, Fuzhou, Fujian, 350108, China

b. State key Laboratory of Structural Chemistry, Fujian Institute of Research on the Structure of Matter, Chinese Academy of Sciences, Fuzhou, Fujian, 350002, China

*CORRESPONDING AUTHOR E-mail: zlin@fjirsm.ac.cn; Tel&Fax: (+086)591-83705474.

Graphical abstract

TOC

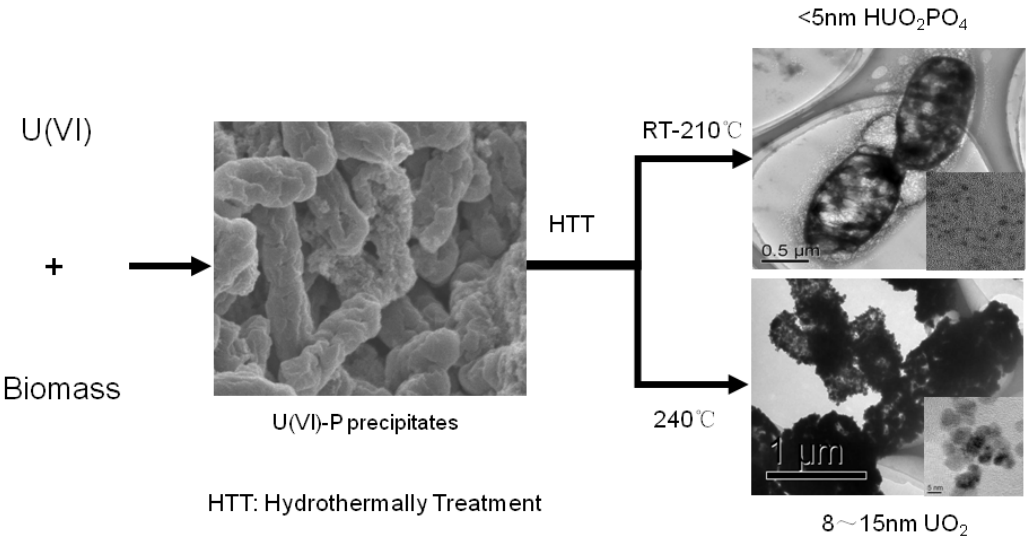

Revealed the hydrothermal conversion rule about amorphous U(VI) to large-size UO_2.

Hydrothermal Growth of Large-Size UO_2 Nano-particles Mediated by Biomass and Environmental Implications

Yangjian Cheng[a,b], *Xinya Xu*[a], *ShungaoYin*[b], *Xiaohong Pan*[b], *Zhi Chen*[b], *and Zhang Lin*[b,*]

a. College of Environment and Resources, Fuzhou University, Fuzhou, Fujian, 350108, China

b. State key Laboratory of Structural Chemistry, Fujian Institute of Research on the Structure of Matter, Chinese Academy of Sciences, Fuzhou, Fujian, 350002, China

*CORRESPONDING AUTHOR E-mail: zlin@fjirsm.ac.cn; Tel&Fax: (+086)591-83705474.

ABSTRACT: One difficult issue that facing environmental scientists is how to convert soluble U(VI) into insoluble U(IV) and recycle it. In the present study, a method, which was widely reported in the literatures, was used to collect the soluble U(VI) using general biomasses (including bacteria and yeast extract), and then a strategy was developed to transform the amorphous uranium-containing precipitates(Uranium-phosphorus Amorphous Compound, UPAC) into large-sized insoluble UO_2 nano-particles. The results show that the biomasses could precipitate more than 90% of the U(VI) (0.42 mmol/L) within 10 min. The maximum precipitation capacity of the biomasses (dry weight) ranged from 120 to 187 mg U/g. The UPAC can be further converted into soluble uranyl phosphate compounds (HUO_2PO_4) at room temperature for 90 days or under the hydrothermal condition at 150 ℃ for 48 h. However, once the hydrothermal temperature was raised to 240°C, insoluble UO_2 nanoparticles around 10 nm could be obtained within 48 h. This work provided a new possibility for the cost-effective preparation of the nuclear fuel (UO_2) with inexpensive raw materials. The mechanism correlation to the transformation of the UPAC into inorganic UO_2 was also discussed here.

KEYWORDS: *UPAC; Large-Size UO_2*; *Nano-particles*; *Hydrothermal Growth*; *Biomass*

1. INTRODUCTION

The demand for uranium has dramatically increased due to the rapid development of atomic energy in recent years. According to International Atomic Energy Agency（IAEA）data, as of April, 2014, a total of 434 nuclear power plants are running in 31 countries around the world, and the total net installed capacity of electrical output is 374 giga watts. The annual requirement of uranium fuel is about 65,900 tonnes world widely. However, for producing each tonne of uranium fuel, about 750 tonnes of 1% uranium ore are required. [1, 2] Therefore, a large amount of uranium-containing wastes (including tailings and slag) are produced during the process of uranium mining and smelting, which seriously pollutes the surface water, groundwater and soil. [3] For example, in the United States alone, there is a huge amount of radionuclide contamination at 120 sites, including more than 3 million cubic meters of buried waste, 1.8 billion cubic meters of affected groundwater and 75 million cubic meters of contaminated sediments. [2, 4] On the other hand, uranium is a well-needed rare resource, and the recycling of uranium becomes an inevitable choice in the future. Therefore, low cost and recyclable strategies for treating soluble U(VI) are in great demand all over the world.

Currently, the main methods for treating uranium-contaminated water include adsorption, ion exchange, and solvent extraction and so on. [5, 6] For example, Yuan *et al.* have used phosphonate-functionalized mesoporous silica for U(VI) sorption from aqueous solution. [7] Zhang *et al.* have studied the removal of uranium(VI) from aqueous systems by heat-treated carbon microspheres. [8] Amaral *et al.* have extracted the thorium and uranium from rare earth elements in monazite sulfuric acid liquor through solvent extraction. [9] John *et al.* have used a polymer inclusion membrane containing di-(2-ethylhexyl) phosphoric acid to extract uranium(VI) from sulfate solutions. [10] However; these methods are costly and inappropriate for treating low-concentration

uranium-contaminated groundwater. Since the low cost of growing bacteria in environment, it is believed that bacteria may play an important role in the in situ remediation of a large amount of low concentration uranium-contaminated groundwater. [11] Previous studies have shown that bacteria can convert the soluble U(VI) into insoluble phase via three approaches: 1) Some bacteria precipitate the uranyl ion via phosphate ligand, which is liberated from the intracellular phosphate bank by phosphatase. [12-14] 2) A few specific bacteria can reduce the soluble U(VI) to UO_2. [15-17] 3) Some bacteria can immobilize U through the formation of uranyl-hydroxide, uranyl-carbonate and calcium-uranyl-carbonate species with functional groups on the cell surfaces. [18-20] However, HUO_2PO_4 precipitation can gradually transform into soluble UO_2CO_3, which can continuously proliferate in the groundwater with high CO_2. [20, 21] Also, the size of biogenic uraninite is commonly less than 3 nm. [17, 21] Such small-size uraninite is mobile and instable, which can be re-oxidized into soluble U(VI) in the oxidative environment. [22] Moreover, the uranium that immobilized by functional groups on the cell surfaces can be re-released into the groundwater with the decomposition of organic matter. [19, 23, 24]

In the preliminary experiments, we also found that the phosphate groups on several common bacterial surface can effectively precipitate the soluble U(VI). Based on this, we try to test the feasibility of the strategy for firstly precipitating the soluble U(VI) by general biomasses, and then converting the precipitates to insoluble large-size UO_2 by using hydrothermal method. Once succeed, on one hand, it will provide a new possibility for the cost-effective preparation of the nuclear fuel (UO_2) with inexpensive raw materials. On the other hand, it can also revealed the mechanism of hydrothermal conversion of uranium-phosphorus amorphous compound (UPAC), as well as the route of environmental migration of U(VI).

2. EXPERIMENTAL SECTION

2.1 Chemicals. All chemicals were of ACS reagent grade and purchased from Sigma-Aldrich Shanghai Trading Co. Ltd. (Shanghai, China). The stock solution of U(VI) was prepared by dissolving uranyl acetate in deionized-distilled water at a concentration of 4.2 mmol/L.

2.2 Cellular origins and cell culture. Three indigenous bacteria were isolated from sandstone-type uranium deposits (underground about 150 m) in the southwestern Turpan-Hami Basin, Xinjiang, China (Latitude: 42.837° North, Longitude: 88.988° East). According to the homology analysis of 16S rDNA sequence, these bacteria were identified as *Clostridium* sp, *B. cereus* and *A. hydrophila*, and their 16S rDNA sequences were deposited in GenBank (Accession No.: GU980195, GU980196 and GU980197). [25] The other two bacteria (*E. coli* and *B. subtilis*) were purchased from the China General Microbiological Culture Collection Center (CGMCC). The yeast extract is available from Oxiod Company.

As an anaerobic bacteria, *Clostridium* sp OH were grown in the HBR medium under the anaerobic condition, and the other four bacteria were cultured in LB medium under the aerobic condition. All the experimental manipulations of *Clostridium* sp OH were carried out inside an anaerobic chamber (Shell Lab, Bacter II, and USA).

2.3 U(VI) precipitation by various biomasses. Cells were harvested when the cell culture reached the stationary phase, and then the cell pellet was washed in Milli-Q water for three times. For the precipitation assay, the cell pellet was re-suspended in Milli-Q water or bicarbonate buffer at a final density of 8×10^8 cells/mL and then amended with 0.42 mmol/L uranyl acetate. Uranium in the precipitation could be determined by deducting the soluble uranium in the supernatant from the initial U(VI) concentration. Soluble U(VI) and total U(VI) were monitored in all the cases.

2.4 Uranium quantification. In order to determine the soluble uranium residual in the supernatant, 2 mL of reaction slurry was passed through a 0.22-μm polycarbonate filter. The filtrate was centrifuged at 8,000 g for 10 min. Subsequently, the soluble U(VI) in the supernatant was acidified and quantified by laser excitation spectrofluorescence with a luminescence spectrometer as previously described. [26, 27] Briefly, uranium samples were diluted (1:30) in 10% phosphoric acid, and the fluorescence of the uranyl-phosphate complex was measured at a wavelength of 515.4 nm. All the measurements were referenced to the fluorescence of the background matrix, the detection limit of this technique was 10 μg/L, and the calibration range bracketed measured U(VI) concentrations. The total uranium was determined using an inductively coupled plasma mass spectrometry (ICP/MS). [27, 28]

2.5 Hydrothermal conversion of the UPAC. The hydrothermal method was used to study the conversion of the UPAC under the hydrothermal condition. Briefly, 0.1 g UPAC (wet weight) and 15 mL double distilled Water was added to the Teflon-lined hydrothermal bomb (bomb volume: about 20 mL). The bombs were stirred for 2 min, and then they were sealed and heated to the room temperature, 60, 90, 120, 150, 180, 210 and 240 °C, respectively. Sampling was performed every month from the samples placed at room temperature, 60 and 90 °C , whereas it was conducted every 24 h from the samples maintained at 120~240 °C. Every temperature series has ten same bombs, every time one of the bombs was taken for analyzing. The heat treatment bomb was cooled down naturally before sampling was performed. The obtained black or yellow sediment was washed with excess pure water and finally air-dried with negative pressure at room temperature for X-ray diffraction (XRD) analysis, transmission electron microscopy (TEM) observation and selective regional electron diffraction (SEAD) analysis.

2.6 SEM, TEM and Atomic Force Microscopy (AFM).

SEM: SEM investigations were performed using a LEO-1530 field emission scanning electron microscope coupled with EDS (Oxford).

TEM: The samples were examined using a JEM-2010 electron microscope at 200 kV. The elemental composition of the precipitations was determined by the energy-dispersive X-ray analysis using a Link EDS (Oxford) attached to a Link light element detector. [29]

AFM: A 5-μL U(VI)-cell (Clostridium sp) suspension was dropped on a freshly cleaved mica substrate and then immediately dried with N_2 gas for 3 min. [30] All the AFM experiments were carried out by a Veeco Multimode NS3A-02 Nanoscope III atomic force microscope. AFM imaging was performed in a tapping mode, and a Si tip from Veeco was used.

2.7 XAFS spectroscopy and XRD. The sample pellet and supernatant were delivered to Shanghai Synchrotron Radiation Facility (SSRF) in a hermetically sealed stainless steel container. U LIII-edge transmission was collected at the SSRF beamlines 14-B using Si (220) double-crystal monochromators detuned to reject higher harmonic intensity. Energy resolution was maintained at less than the 8.67 eV natural line width of the uranium L-3 edge using vertical slits. Samples were analyzed at 77 K. The analysis of the experimental XAFS spectra was performed by WinXAS3.1. [31]

For XRD analysis, the precipitate was collected on a Whatman filter paper (no. 5), dried with N_2, and ground to a fine powder with a mortar and pestle. The randomly oriented powder was mounted on a glass slide with amyl acetate. The X-ray diffractometer was equipped with a graphite monochrometer and a nickel filter, and Cu Kα radiation was used at a wavelength of 1.5418 Å (0.15418 nm). The scan rate was 1 ° (2theta)/min, with a soller-slit of 10 and a receiving slit of 0.25 °. The average crystallite size was calculated from the peak broadening using the Scherrer equation. [32]

3. RESULTS AND DISCUSSION

3.1 **Rapid precipitation of soluble U(VI) mediated by biomass.** Studies have shown that the phosphate, carboxyl and amino groups on the bacterial surface may coordinate with U(VI) to promote the precipitation of U(VI)[12, 18, 23]. In order to confirm the universality of this transformation, we investigated the precipitation of U(VI) ion using a variety of representative biomasses. As revealed in Table 1, no matter what kind of biomass was used, when 100 mg/L biomass (dry weight) was added to 0.42 mmol/L soluble U(VI), more than 90% of soluble U(VI) could be precipitated within 10 min. However, according to the biomass type, the precipitation capacity varied slightly. For these six kinds of biomasses, the maximum precipitation capacity ranged from 120 to 187 mg U/g (dry weight). There are similar to other's studies, such as the maximum precipitation capacity of the *Citrabacter* N14. and *E. coli* DH5α (phoN) are 91 and 151 mg U/g (dry weight), respectively. [33]

Table 1 The interaction of U(VI) with a variety of biomasses

Biomass	Gram type	Residual U(VI) concentration (μmol/L)[a], N=3	Removal ratio (%)	Amount of precipitation per gram biomass (mg/g)[b]
A. hydrophila	G^-	32.0±0.5	92.4	121
B. cereus	G^+	7.9±0.7	98.12	185
B. subtilis	G^+	5.8±0.8	98.61	187
Clostridium sp. OH	G^+	9.3±0.3	97.79	176
E. coli	G^-	38.6±0.2	90.8	120
Yeast extra.	/	15.3±0.6	96.35	168

Note: a. The initial concentration of uranium was 0.42 mmol/L when the biomass was added, the U(VI) in the supernatant was the average of three experiments. b. To calculate the

maximum precipitation capacity, the precipitate was collected by centrifugation and then reintroduced to the uranium solution until an excess of uranium.

The SEM was further used to analyze the U precipitates that collected by *Clostridium* sp. OH. It reveals that a lot of precipitate deposited around the bacteria (Fig. 1a). EDS quantitative data showed that the molar ratio of uranium and phosphate ions was 1:1.36 in the amorphous uranium (Fig. 1b). The signal of the nitrogen was not detected by EDS. Therefore, the phosphate group may probably play a dominant role in the process of U(VI) precipitation. And the precipitates are called here as uranium-phosphorus amorphous compounds (UPAC).

The above-mentioned uranium-containing precipitates (including biomasses) were washed with water and air-dried at room temperature for XRD and XAFS analysis. The XRD result indicated that they were amorphous (Fig. 1c). X-ray absorption near edge structure (XANES) showed that the uranium L-3 edge of precipitates was consistent with that of uranyl acetate, and with 12-eV difference compared to uraninite (Fig. 1d). This indicated that the valence state of the amorphous uranium was still hexavalent, suggesting that the redox process did not occur in this condition. Due to the bacteria, which were selected in our experiments, are not the metal reducing bacteria or sulfate-reducing bacteria. The extent of U(VI) reduction depended on the bacterial species and the experimental conditions. [34] It was reported that the dissimilatoty metal reducing bacteria, such as the *Anaeromyxobacter dehalogenans* strain K, *Geobacter sulfurreducens* strain PCA, and *Shewanella putrefaciens* strain CN-32, can reduce the U(VI) to U(IV) in some extent at low temperature condition. [34]

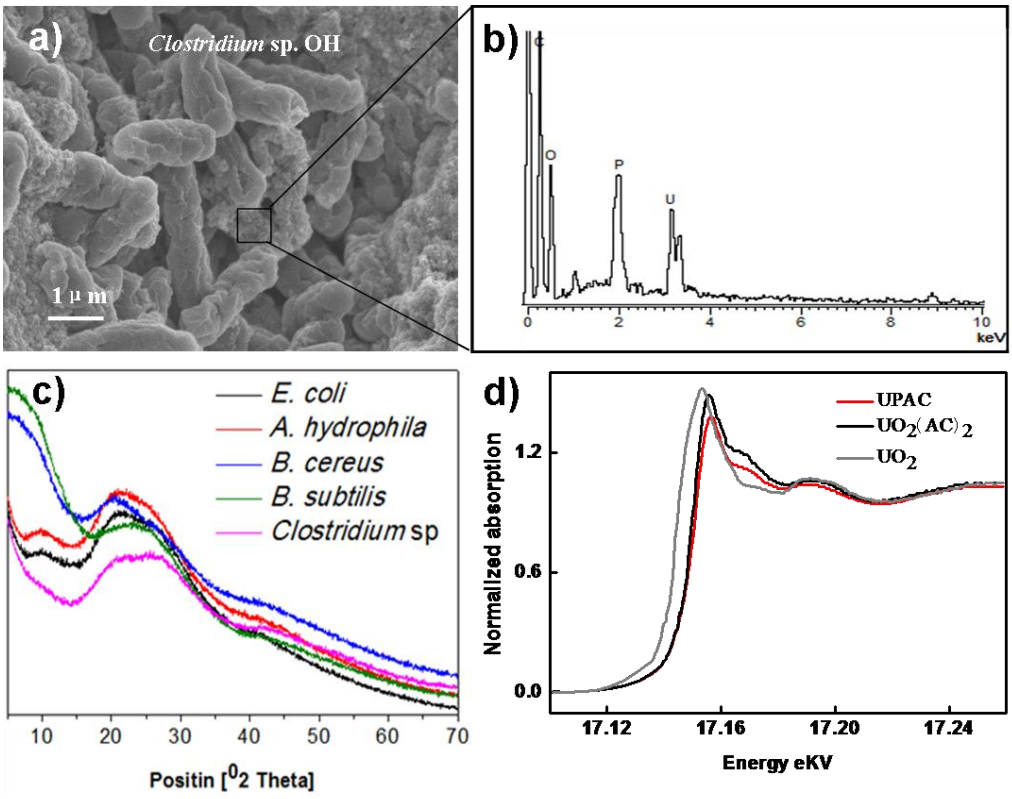

Figure 1. a. SEM analysis of the U(VI) precipitates that collected by *Clostridium* sp OH. b. EDS analysis of the area that containing precipitants (the area is indicated by a black square in Figure 1a). c. XRD analysis of a series of uranium-containing precipitates; d. The comparison of XANES spectroscopy of the U precipitates that collected by *Clostridium* sp. OH with two standard compounds (uranyl acetate--$UO_2(Ac)_2$ and UO_2).

3.2 Conversion of UPAC to HUO_2PO_4. For studying the possible transformation states of U(VI) that mediated by biomass, at first, we try to store the above-mentioned UPAC at room temperature for 90 days or hydrothermally treating it at 150 ℃ for 48h (Table 2). U precipitates that collected by *Clostridium* sp. OH was taken as a special case for further analysis. XRD results showed that the UPAC could be converted into the uranyl phosphate compounds (HUO_2PO_4) at room temperature with time (Table 2; Fig. 2a).

Table 2 Phase composition of the sediments after treatment at different temperatures for different times.

T [Days]	RT	60	90	120	150	180	210	240 (℃)
1	□	□	□	□	□△	△	△	△■
2	--	--	--	□	△	△	△	■
3	--	--	--	□	△	△	△	■
4	--	--	--	□	△	△	△	■
5	--	--	--	□	△	△	△	■
6	--	--	--	□△	△	△	△	■
30	□	□	△	--	--	--	--	--
60	□	△	△	--	--	--	--	--
90	□△	△	△	--	--	--	--	--
120	△	△	△	--	--	--	--	--

Note: 1). □: UPAC; △: HUO_2PO_4; ■:UO_2; RT: Rome temperature; --: Non-Detected;

2). □ △ and △ ■ represents both phases, the conversion is incomplete.

AFM observation showed that a large amount of precipitates were attached to the bacterial surface, which is very similar to the UPAC before treatment (Fig. 2a insert). Under the hydrothermal condition at 150 ℃ for 48 h, XRD results showed that the UPAC still can only convert into HUO_2PO_4 (Table 2, Fig. 2b). TEM observation showed that the outline of the bacteria was still clearly visible observed after treating at 150 ℃ for 48 h (Fig. 2c). SEAD confirmed that the nano-particles that attached on the surface of bacteria were HUO_2PO_4 (Fig. 2c insert). Moreover, as shown in Fig. 2d, HR-TEM observation revealed that the size of the nano-particles was less than 5 nm, no large-size and insoluble uranium-containing phase, such as UO_2

were observed. However, it is worth mentioning that the conversion time from UPAC to HUO_2PO_4 could be greatly reduced at hydrothermal condition (only 48 h at 150 ℃). Same was the case for the other four types of biomasses (data not shown here).

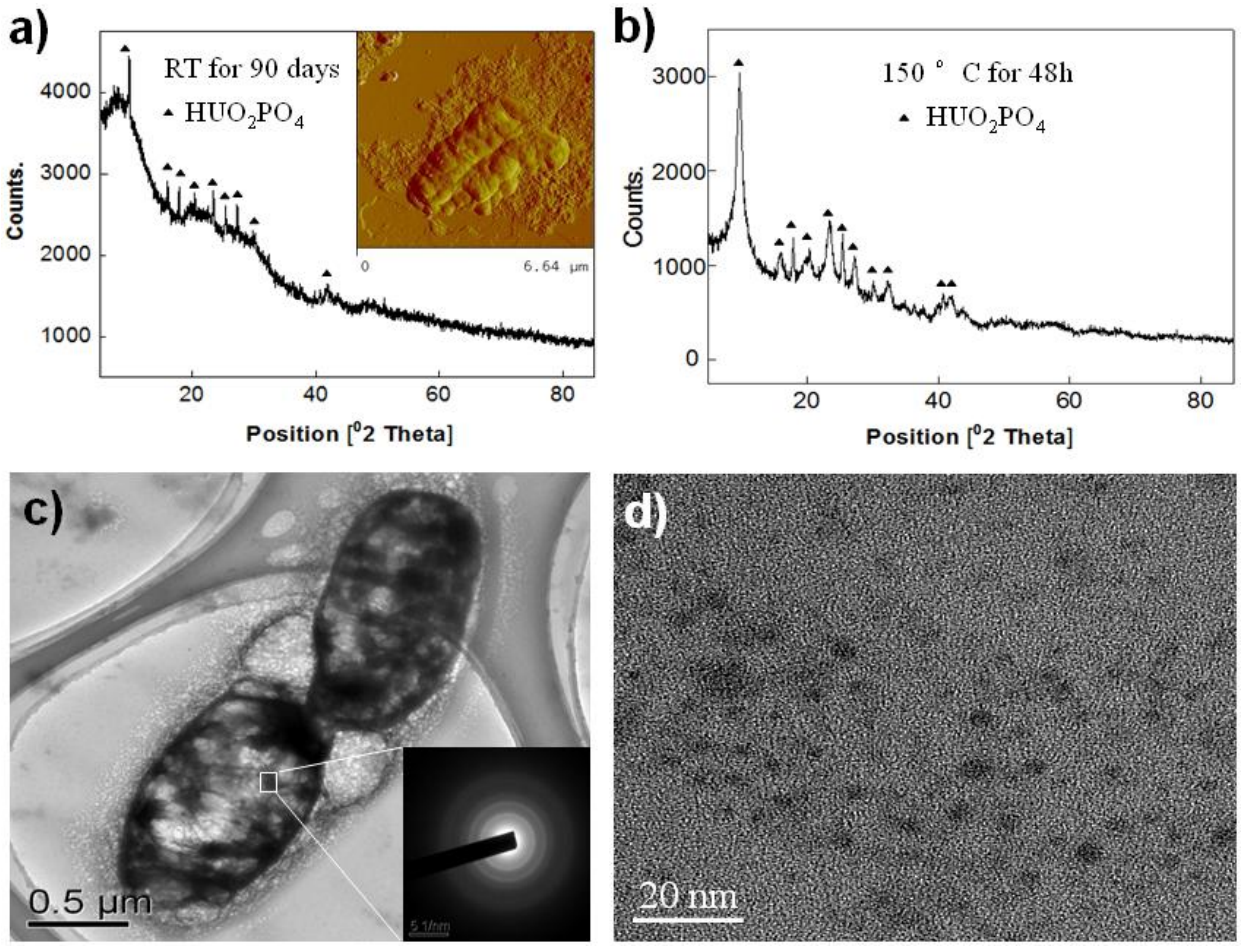

Figure 2. The transformation of *Clostridium* sp. mediated UPAC at room temperature for 90 days or under hydrothermal condition (150 ℃ for 48 h). a. XRD analysis and AFM observation (Inset) of the sample that treated at room temperature for 90 days. b. XRD analysis of the sample that treated at 150 ℃ for 48h. c. TEM observed the sample that treated under the hydrothermal condition at 150 ℃ for 48 h. Inset: Application of SEAD to analysis of the area that indicated by square in Figure 2c. d. HR-TEM observation of the square of Fig.2c.

3.3 Conversion of the UPAC.

For effectively converting UPAC into aiming insoluble phase, we tried to elevate the hydrothermal temperature to 240 °C. After freeze-drying, the samples were analyzed by TEM and XRD. Fig. 3a and 3b were the TEM images of the transformed UPAC. It revealed that, after hydrothermal conversion at 240°C for 48 h, the outline of the bacteria was clearly visible under the TEM without negative stain; also, a large number of nano-particles were attached to the bacterial surface. As shown in Fig. 3 inserts, HR-TEM revealed that the size of the nano-particle was about 10 nm, which is coincident with the results from XRD analysis.

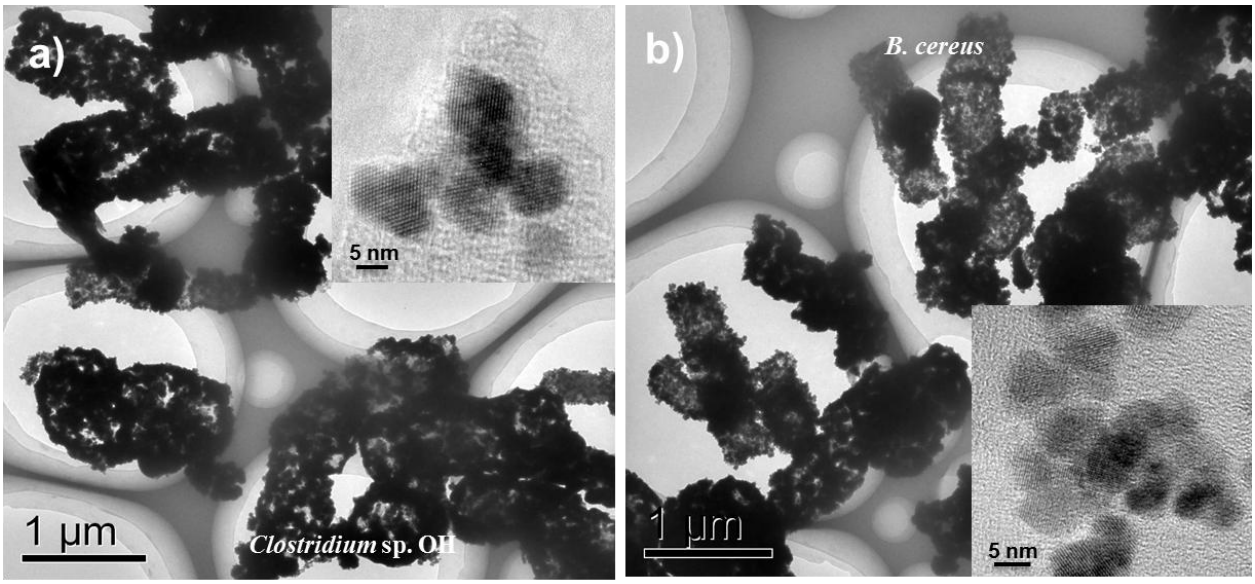

Figure 3. HRTEM observation of the samples after hydrothermal treatment at 240 °C for 48 h. a) Collected by *Clostridium* sp OH; b) collected by *B. cereus*.

X-ray diffraction (XRD) analysis revealed that all diffraction peaks could be well indexed as standard uraninite structure (Fig. 4 a). It indicates that the UPAC phase is changed completely into UO_2 when hydrothermal temperature elevated to 240 °C for 48 h （Table 2）. According to Scherrer equation, the sizes of the produced UO_2 was about 8-13 nm for the six kinds of

biomasses. Not only the gram negative bacteria but also the gram positive bacteria all could completely convert the UPAC to UO_2 at 240 °C, it suggests that the conversion is universal (Fig. 4 a).

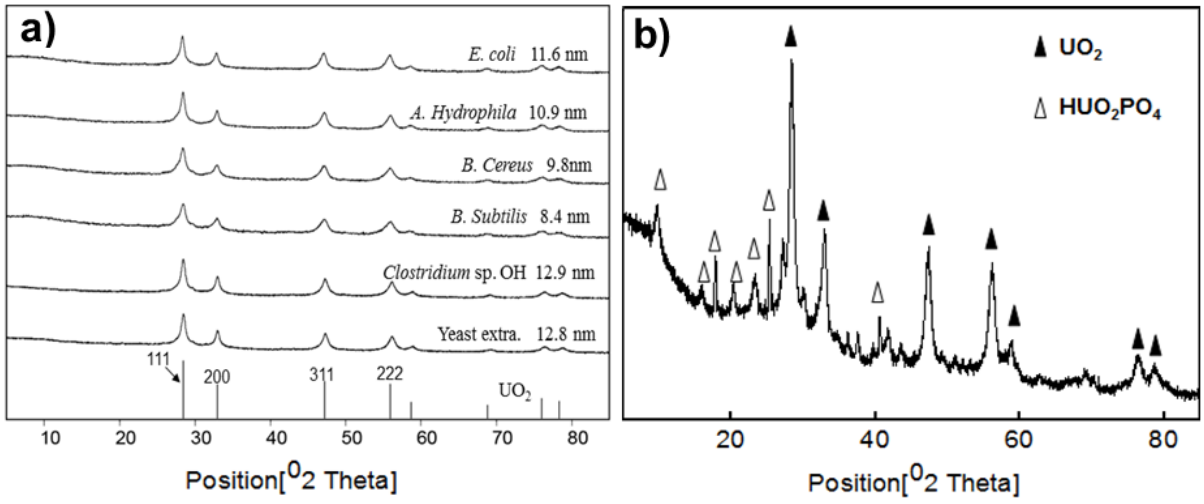

Figure 4. XRD spectra of UPAC after hydrothermally treated. a) UPAC treated at 240 °C for 48 h. b) XRD data showed that the carbonate ions affected the stability of the uranyl phosphate compounds.

3.4 Stability of the produced UO_2 nano-particles. It is known that the material stability depends on its particle size, surface state, composition and some other factors.[35-37] Previous work revealed that the direct reduction of U(VI) by the microorganisms could producing UO_2 particle with size no more than 3nm. Small-size UO_2 particles can not only easily migrate with water,[17, 21] but also is not stable in environment and easy to be reoxidized.[38, 39] Thus relatively big size of the produced UO_2 should be the goal of this investigation. Here, using the sample collected by *Clostridium* sp. OH. As the representative, we performed the time series experiments (48, 72 and

96 h) under the hydrothermal condition at 240 °C, for disclosing the size evaluation rule of the sample during hydrothermal treatment. It revealed that the UO_2 was 9.8, 10.7 and 10.5 nm at the three time points of 48, 72 and 96 h, respectively. It revealed that the growth of the nano-particles almost reached equilibrium at 48 h, suggesting that a relatively stable size of about 10 nm could be obtained under certain hydrothermal conditions. Such large-size uraninite should be relatively stable for long-term in the environment.[17, 38] It implied that the UPAC formed in the environment could be converted into the UO_2 nano-particles under the certain environmental conditions, such as volcanic eruptions or geothermal activity zone, which indicate a possible route of bioremediation of soluble uranium. However, the long-term stability of the relatively large-size uraninite is uncertain, especially if surrounding become oxic and it become susceptible to oxidation back to the soluble U(VI). [34, 38]

3.5 Carbonate effect on the hydrothermal transformation. Previous work has shown that the uranyl phosphate compounds can be dissolved and converted into uranyl ion at the high concentration of carbonate ions, this finding was also confirmed in our experiments.[40, 41] If formation of uranyl phosphate compounds then to add the biomass to this system, uranyl phosphate compounds cannot be converted into the uraninite under the hydrothermal condition at 240 °C for 48 h. However, if the carbonate ions existed in the above system, XRD data indicated that the uraninite appeared after the hydrothermal treatment (Fig. 4 b). It implied that the uranyl phosphate may convert to soluble uranyl carbonate in the presence of carbonate ions,[18, 41] and then soluble uranyl carbonate may reconvert to uraninite in the biomass-mediated hydrothermal conversion (240 °C for 48h). Due to the instability of uranyl phosphate compound in the environment, it is not conducive to the *in situ* remediation of uranium contamination.

It was reported that the reduction extent of the same mass of HUP (HUO_2PO_4) to U(IV) was consistently greater with the biogenic than with the abiotic material under the same experimental

conditions. A greater extent of HUP reduction was observed in the presence of bicarbonate in solution, whereas a decreased extent of HUP reduction was observed with the addition of dissolved phosphate. These results indicate that the extent of U(VI) reduction is controlled by dissolution of the HUP phase. [34] This result is consistent with our result that the carbonate affects on the hydrothermal transformation from HUP to uraninite.

4. CONCLUSION

On the whole, above results suggested that the biomass could not only quickly co-precipitate the soluble uranyl ion, but also mediate the conversion of uranium from U(VI) into UO_2 nano-particles with relatively large size. As shown in Fig. 5, it took 90 days to convert the UPAC into uranyl phosphate compounds at room temperature. If the hydrothermal temperature was raised to 150 °C, the conversion time could be reduced to 48 h. However, the UPAC could be reduced into UO_2 within 48 h if the hydrothermal temperature was raised to 240 °C. This work provided a new way to recycle uranium resource with inexpensive raw materials.

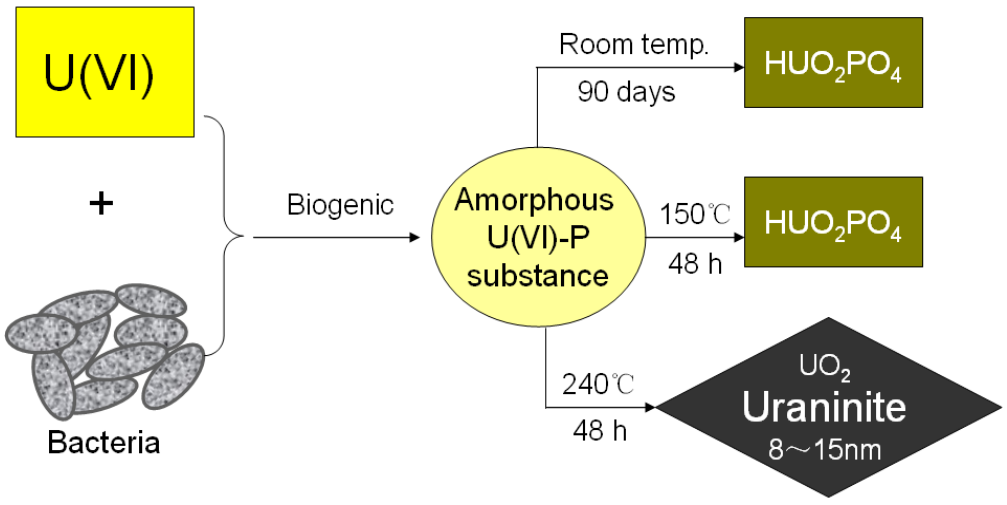

Figure 5. An overview of the general routes for converting soluble uranyl ion into other phases.

ACKNOWLEDGMENT

Financial support for this study was provided by the National Basic Research Program of China (973 Program) (2014BC846003, 2010CB933501), the National Natural Science Foundation for Distinguished Young Scholars (21125730) and the National Natural Science Foundation of China (41372346, 21477129).

REFERENCES

1. A. Abdelouas, *Elements*, 2006, **2**, 335-341.
2. Q. H. Hu, J. Q. Weng and J. S. Wang, *J Environ Radioactiv*, 2010, **101**, 426-437.
3. A. J. Bednar, V. F. Medina, D. S. Ulmer-Scholle, B. A. Frey, B. L. Johnson, W. N. Brostoff and S. L. Larson, *Chemosphere*, 2007, **70**, 237-247.
4. Y. J. Cheng, H. Y. Holman and Z. Lin, *Elements*, 2012, **8**, 107-112.
5. M. Gavrilescu, L. V. Pavel and I. Cretescu, *J Hazard Mater*, 2009, **163**, 475-510.
6. M. Charbonneau, *MMG 445 Basic Biotech*, 2009, **5**, 6.
7. L. Y. Yuan, Y. L. Liu, W. Q. Shi, Y. L. Lv, J. H. Lan, Y. L. Zhao and Z. F. Chai, *Dalton T*, 2011, **40**, 7446-7453.
8. X. Zhang, J. Wang, R. Li, Q. Liu, L. Li, J. Yu, M. Zhang and L. Liu, *Environ Sci Pollut Res Int*, 2013, **20**, 8202-8209.
9. J. C. B. S. Amaral and C. A. Morais, *Miner Eng*, 2010, **23**, 498-503.
10. A. M. St John, R. W. Cattrall and S. D. Kolev, *J Membrane Sci*, 2010, **364**, 354-361.
11. J. U. Lee, S. M. Kim, K. W. Kim and I. S. Kim, *Chemosphere*, 2005, **59**, 147-154.
12. L. E. Macaskie, R. M. Empson, A. K. Cheetham, C. P. Grey and A. J. Skarnulis, *Science*, 1992, **257**, 782-784.
13. N. Renninger, R. Knopp, H. Nitsche, D. S. Clark and J. D. Keasling, *Appl Environ Microb*, 2004, **70**, 7404-7412.
14. R. J. Martinez, M. J. Beazley, M. Taillefert, A. K. Arakaki, J. Skolnick and P. A. Sobecky, *Environ Microbiol*, 2007, **9**, 3122-3133.

15. Y. T. Liang, J. D. Van Nostrand, L. A. N'Guessan, A. D. Peacock, Y. Deng, P. E. Long, C. T. Resch, L. Y. Wu, Z. L. He, G. H. Li, T. C. Hazen, D. R. Lovley and J. Z. Zhou, *Appl Environ Microb*, 2012, **78**, 2966-2972.

16. D. R. Lovley, E. J. P. Phillips, Y. A. Gorby and E. R. Landa, *Nature*, 1991, **350**, 413-416.

17. Y. Suzuki, S. D. Kelly, K. M. Kemner and J. F. Banfield, *Nature*, 2002, **419**, 134-134.

18. J. D. Kubicki, G. P. Halada, P. Jha and B. L. Phillips, *Chem Cent J*, 2009, **3**.

19. A. Barkleit, H. Moll and G. Bernhard, *Dalton T*, 2009, 5379-5385.

20. D. A. Fowle, J. B. Fein and A. M. Martin, *Environ Sci Technol*, 2000, **34**, 3737-3741.

21. J. R. Bargar, R. Bernier-Latmani, D. E. Giammar and B. M. Tebo, *Elements*, 2008, **4**, 407-412.

22. M. Ginder-Vogel, B. Stewart and S. Fendorf, *Environ Sci Technol*, 2010, **44**, 163-169.

23. J. R. Haas, T. J. Dichristina and R. Wade, *Chem Geol*, 2001, **180**, 33-54.

24. B. Jagetiya and A. Sharma, *Chemosphere*, 2013, **91**, 692-696.

25. Z. Chen, Y. J. Cheng, D. M. Pan, Z. X. Wu, B. Li, X. H. Pan, Z. P. Huang, Z. Lin and X. Guan, *Geomicrobiol J*, 2012, **29**, 255-263.

26. Q. Wu, R. A. Sanford and F. E. Loffler, *Appl Environ Microb*, 2006, **72**, 3608-3614.

27. S. D'Ilio, N. Violante, O. Senofonte, C. Majorani and F. Petrucci, *Anal Methods-Uk*, 2010, **2**, 1184-1190.

28. E. A. Ough, B. J. Lewis, W. S. Andrews, L. G. I. Bennett, R. G. V. Hancock and P. A. D'Agastino, *Health Phys*, 2006, **90**, 494-499.

29. B. Li, D. M. Pan, J. S. Zheng, Y. J. Cheng, X. Y. Ma, F. Huang and Z. Lin, *Langmuir*, 2008, **24**, 9630-9635.

30. C. P. Yang, Y. J. Cheng, X. Y. Ma, Y. Zhu, H. Y. Holman, Z. Lin and C. Wang, *Langmuir*, 2007, **23**, 4480-4485.

31. T. Ressler, *J Synchrotron Radiat*, 1998, **5**, 118-122.

32. W. Z. Liu, F. Huang, Y. J. Wang, T. Zou, J. S. Zheng and Z. Lin, *Environ Sci Technol*, 2011, **45**, 1955-1961.

33. G. Basnakova, E. R. Stephens, M. C. Thaller, G. M. Rossolini and L. E. Macaskie, *Appl Microbiol Biotechnol*, 1998, **50**, 266-272.

34. X. Rui, M. J. Kwon, E. J. O'Loughlin, S. Dunham-Cheatham, J. B. Fein, B. Bunker, K. M. Kemner and M. I. Boyanov, *Environ Sci Technol*, 2013, **47**, 5668-5678.

35. E. Schofield, A. Mehta, S. Webb, K. U. Ulrich, D. E. Giammar, J. O. Sharp, H. Veeramani, R. Bernier-Latmani, S. Conradson, D. Clark and J. R. Bargar, *Geochim Cosmochim Ac*, 2008, **72**, A838-A838.

36. K. U. Ulrich, E. J. Schofield, J. R. Bargar, J. O. Sharp, H. Veeramani, R. Bernier-Latmani, A. Singh and D. E. Giammar, *Geochim Cosmochim Ac*, 2008, **72**, A966-A966.

37. I. Perelshtein, G. Applerot, N. Perkas, E. Wehrschetz-Sigl, A. Hasmann, G. M. Guebitz and A. Gedanken, *Acs Appl Mater Inter*, 2009, **1**, 363-366.

38. T. Borch, R. Kretzschmar, A. Kappler, P. Van Cappellen, M. Ginder-Vogel, A. Voegelin and K. Campbell, *Environ Sci Technol*, 2010, **44**, 15-23.

39. S. Chinni, C. Anderson, K. U. Ulrich, H. Veeramani, J. O. Sharp, D. E. Giammar, R. Bernier-Latmani and B. M. Tebo, *Geochim Cosmochim Ac*, 2008, **72**, A158-A158.

40. Z. P. Zheng, J. M. Wan, X. Y. Song and T. K. Tokunaga, *Colloid Surface A*, 2006, **274**, 48-55.

41. S. Kerisit and C. X. Liu, *Geochim Cosmochim Ac*, 2010, **74**, 4937-4952.